Electronic Supplementary Material (ESI) for Energy & Environmental Science.

Supplementary Information

Multi-anionic and -cationic compounds: New high entropy materials for advanced Li-ion batteries

Q. Wang et al.

$$S_{\text{config}} = -\mathrm{R}[(\sum_{i=1}^{N} x_i \ln x_i)_{\text{cation site}} + (\sum_{j=1}^{M} x_j \ln x_j)_{\text{anion site}}]$$

Equation S1. Calculation of S_{config} for $Li_{0.5}(Co_{0.1}Cu_{0.1}Mg_{0.1}Ni_{0.1}Zn_{0.1})O_{0.5}F_{0.5}$ as an example: $S_{\text{config}} = -\mathrm{R}(((0.5\ln0.5)+(0.1\ln0.1)+(0.1\ln0.1)+(0.1\ln0.1)+(0.1\ln0.1)+(0.1\ln0.1))_{\text{cations}} + ((0.5\ln0.5)+(0.5\ln0.5))_{\text{anions}}) = -\mathrm{R}\,((-1.5)_{\text{cations}} + (-0.69)_{\text{anions}})) = 2.19\ \mathrm{R}$

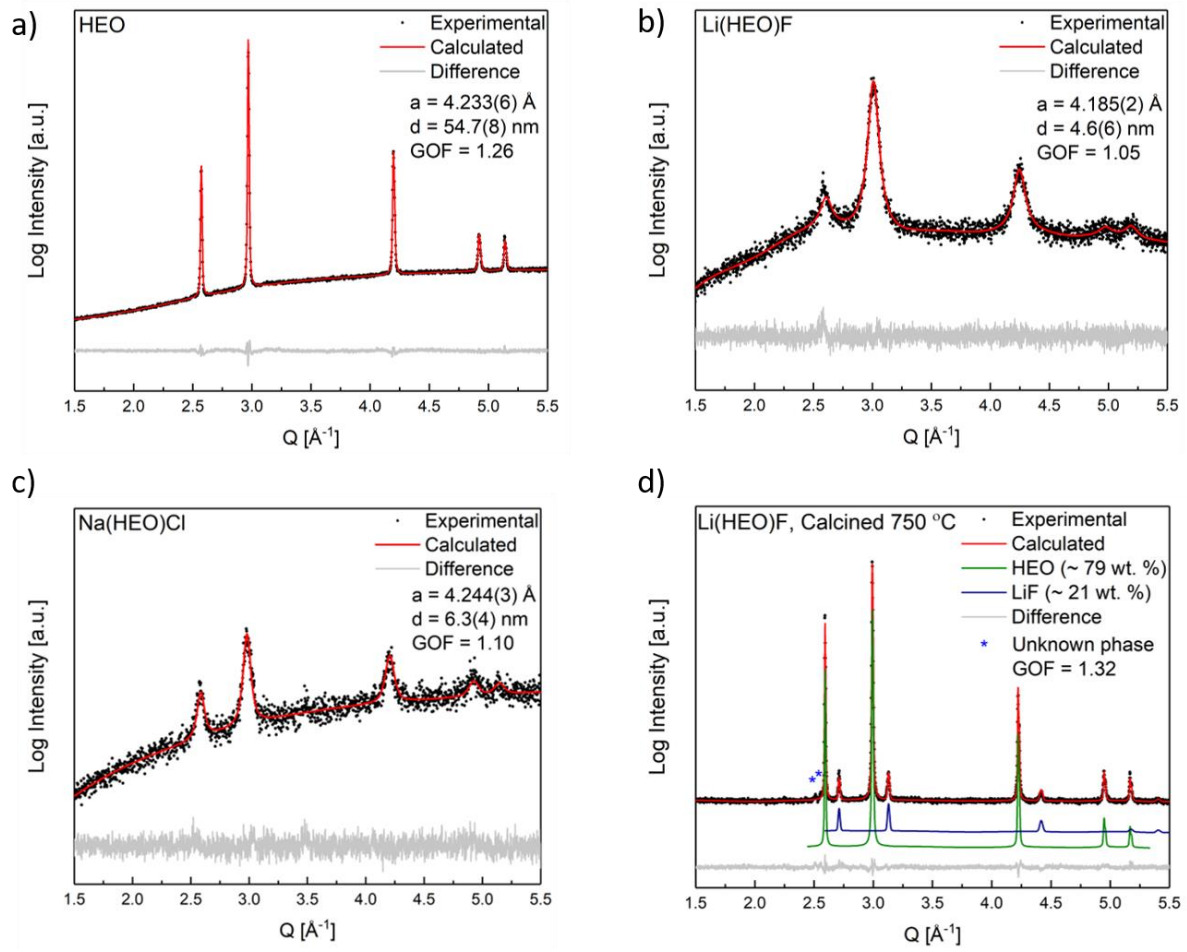

Figure S1. XRD patterns and the corresponding Rietveld fits for (a) HEO, (b) Li(HEO)F, (c) Na(HEO)Cl and (d) Li(HEO)F calcined at 750 °C for 2 h. Refined lattice parameter *a*, crystallite size *d* and goodness of fit GOF are given in the figures.

Table S1. Rietveld refinement results for Li(HEO)F. The XRD pattern was fitted using a single-phase rock-salt structure. Note that the structural file has been modified by taking into account the results from XPS and ICP.

Phase	rock-salt				
Space group	*Fm*−3*m*				
Cell volume (Å^3)	74.13(10)				
Density (g cm^{-3})	4.275(6)				
Lattice parameter *a* (Å)	4.185(2)				
Site	*x*	*y*	*z*	Atom	Occupation
4a (cation)	0.00000	0.00000	0.00000	Ni^{+2}	0.039(13)
				Co^{+2}	0.096(14)
				Mg^{+2}	0.110(0)
				Zn^{+2}	0.100(0)
				Cu^{+1}	0.090(1)
				Ni^{+3}	0.068(13)
				Co^{+3}	0.011(14)
				Li^{+1}	0.043(2)
4b (anion)	0.50000	0.50000	0.50000	O^{-2}	0.55(0)
				F^{-1}	0.45(7)

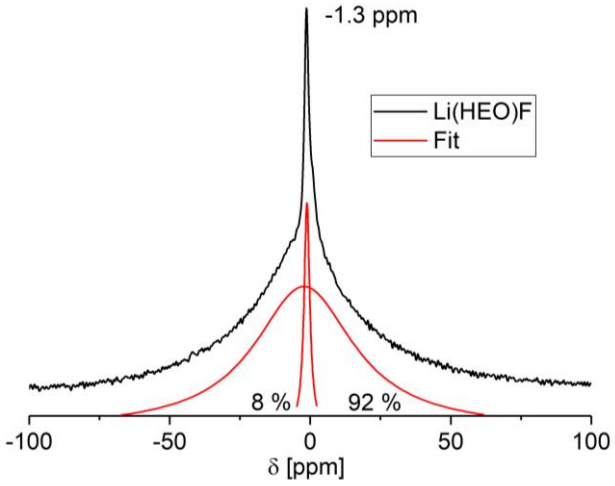

Figure S2. Voigt fit of ^{7}Li-MAS-NMR spectrum indicating the presence of about 8% unreacted LiF in Li(HEO)F.

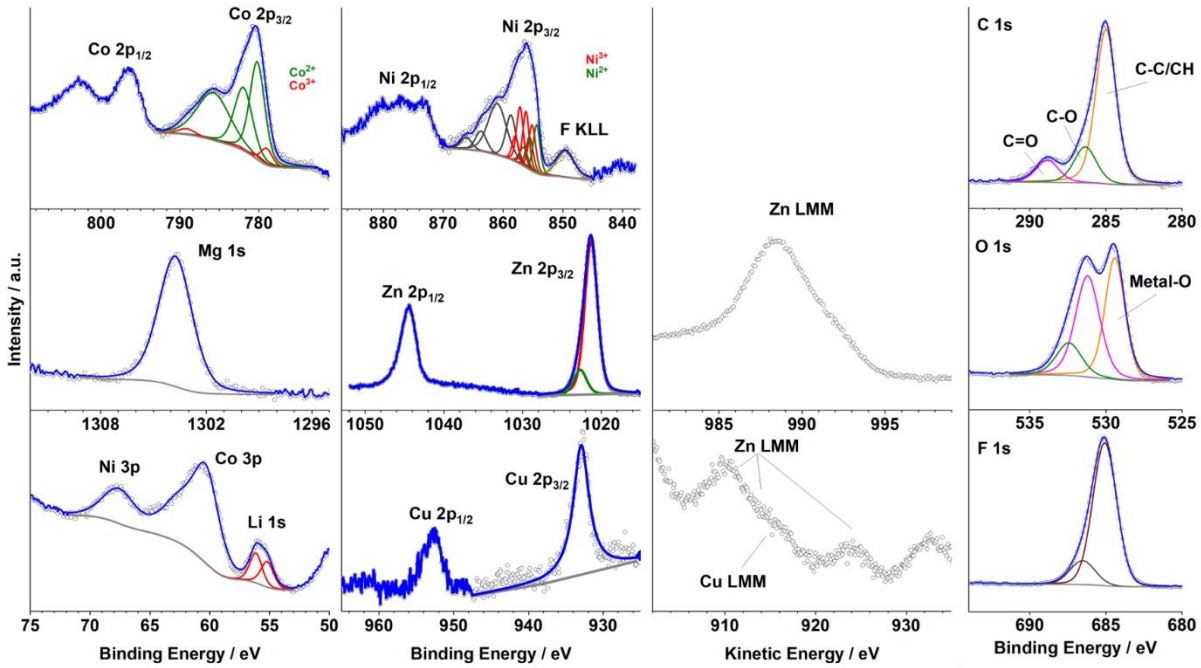

Figure S3. XPS spectra of the Co 2p, Ni 2p, Mg 1s, Zn 2p, Li 1s, Cu 2p, C 1s, O 1s and F 1s core level regions as well as Cu LMM and Zn LMM Auger spectra for Li(HEO)F. The Zn $2p_{3/2}$ at 1021.3 eV and Zn LMM at 988.6 eV indicate the presence of Zn^{2+}.[1] The Cu 2p spectrum can be assigned to Cu^{1+} ions (with Cu $2p_{3/2}$ at 933 eV).

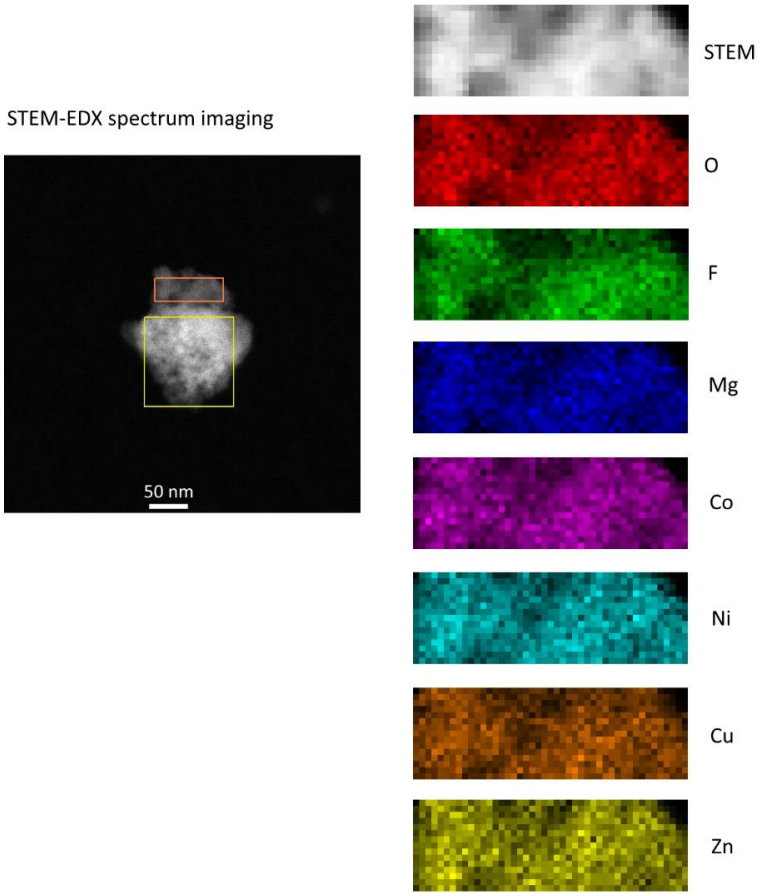

Figure S4. STEM-EDX mapping of Li(HEO)F.

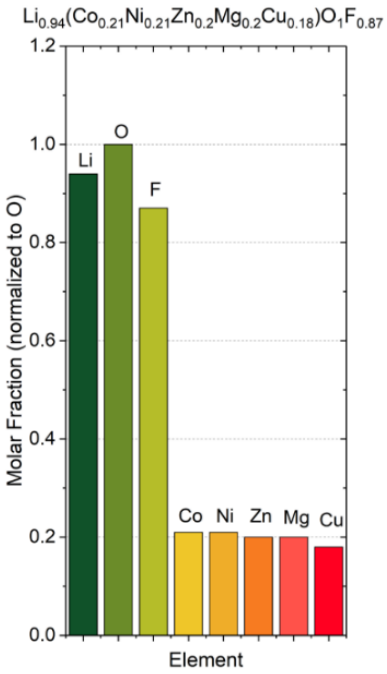

Figure S5. Overall composition of Li(HEO)F from ICP-OES, NMR and EDX.

Note S1. ICP-OES elemental analysis was accomplished using four different calibrated solutions and two internal standards (Na, Sc). The oxygen content was analyzed via carrier gas hot extraction (CGHE). To this end, a commercial oxygen/nitrogen analyzer TC600 (LECO) was used. The oxygen concentration was calibrated using the certified standard KED 1025. Both the standard and the sample were weighed with a mass ranging from 1 to 2 mg (±0.05 mg accuracy) in Sn crucibles (9-10 mm), followed by wrapping. The samples were then put together with a Sn pellet (about 200 mg) into a Ni crucible and loaded in an outgassed (5500 W) high-temperature graphite crucible. The evolving gases CO_2 and CO were swept out by He as an inert carrier gas and measured by infrared detectors. The fluorine content was analyzed using an ion-selective electrode (perfectION, Mettler Toledo). The digestions were diluted and adjusted to a pH between 5 and 8 using both 5 M NaOH solution and TISAB (total ionic strength adjustment buffer) solution. The fluorine concentration was determined via the method of standard addition. The amount of Li was determined from combined ICP-MS and NMR data. The ICP-MS results for the as-prepared Li(HEO)F are given below. Because unreacted LiF was observed by NMR, 8% of lithium and fluorine were subtracted from the ICP-MS data, leading to a composition of $Li_{0.94}(Co_{0.21}Ni_{0.21}Zn_{0.2}Mg_{0.2}Cu_{0.18})O_1F_{0.87}$.

Element	Mol. ratio to oxygen
Li	1.02
O	1
Mg	0.2
Co	0.21
Ni	0.21
Cu	0.18
Zn	0.2
F	0.99

Note S2. For HEOs, a conversion reaction takes place, which partially reduces the transition metal species to their elemental state. The reaction occurs at relatively low potentials; no electrochemical activity at higher potentials (like for Li(HEO)F) is observed. This can be seen from **Figure 4**, comparing the redox reactions for HEO and Li(HEO)F. The Li(HEO)F compound reveals an insertion mechanism, where Li is inserted/extracted into/from the lattice without inducing significant structural changes. This reaction occurs at a much higher potential, following the equation $V(\mathrm{x}) = -\Delta G / (x_\mathrm{j} - x_\mathrm{i}) \cdot F$, where $V(\mathrm{x})$ is the average equilibrium voltage, ΔG the difference in Gibbs free energy, x_j and x_i are the borders of the miscibility gap of the insertion reaction and F represents the Faraday constant. The latter equation indicates that even if an insertion type reaction would be possible in the HEO case, the electrochemical potential of the oxyfluoride material would be higher (because of the higher free energy of formation of fluoride compounds in general [e.g., CoO ≈ 240 kJ/mol vs. CoF_2 ≈ 670 kJ/mol)]. This can be explained as follows: According to the crystal field concept,[4] the redox potential of insertion electrode materials is governed by the ionocovalency of the M-X bond (M: transition metal, X: oxygen, fluorine or sulfur). The more ionic the bonding, the higher the potential. The highly ionic M-F bond stabilizes the energy of the antibonding M-*d* orbitals of the transition metal ion, thus increasing the voltage at which the lithium insertion reaction occurs, while the opposite is observed for elements with lower electronegativity such as sulfur.[5,6] Therefore, the incorporation of fluorine into the original rock-salt type $Co_{0.2}Cu_{0.2}Mg_{0.2}Ni_{0.2}Zn_{0.2}O$ results in a relatively high working potential of 3.4 V vs. Li^+/Li.

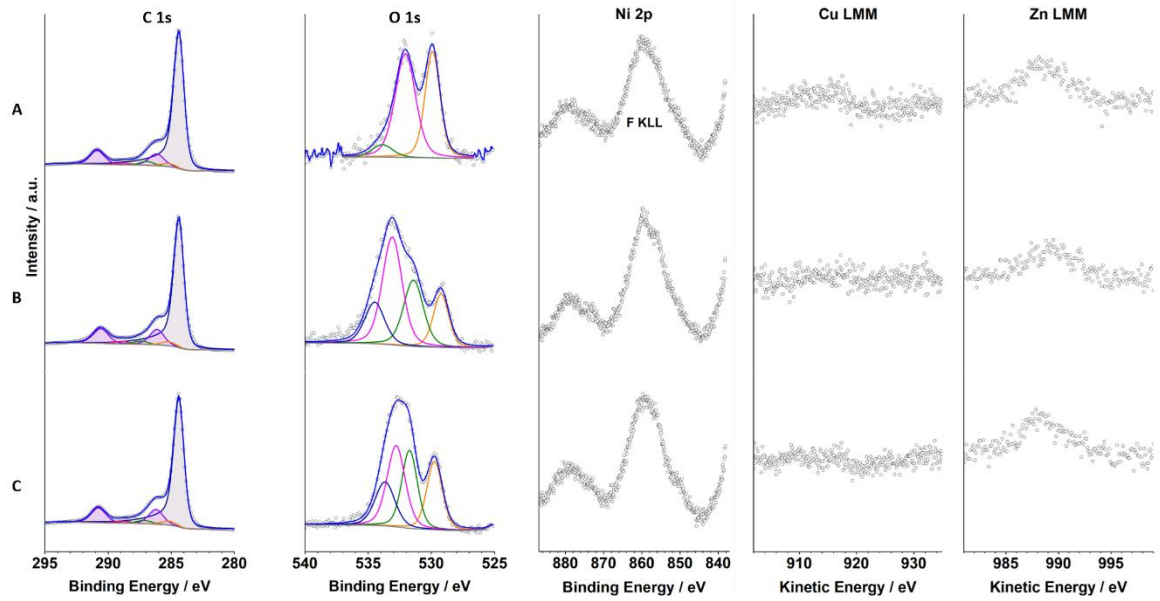

Figure S6. XPS spectra of the C 1s, O1s and Ni 2p core level regions as well as Cu LMM and Zn LMM Auger spectra for Li(HEO)F in (A) pristine state, (B) delithiated state and (C) lithiated state.

References

1 Z. Zhao, G. Tian, A. Sarapulova, V. Trouillet, Q. Fu, U. Geckle, H. Ehrenberg and S. Dsoke, *J. Mater. Chem. A*, 2018, **6**, 19381–19392.

2 V. Kumar, C. R. Mariappan, R. Azmi, D. Moock, S. Indris, M. Bruns, H. Ehrenberg and G. Vijaya Prakash, *ACS Omega*, 2017, **2**, 6003–6013.

3 C. R. Mariappan, V. Kumar, R. Azmi, L. Esmezjan, S. Indris, M. Bruns and H. Ehrenberg, *CrystEngComm*, 2018, **20**, 2159–2168.

4 J. B. Goodenough, in *Advances in Lithium-Ion Batteries*, Springer US, Boston, MA, 2002, pp. 135–154.

5 E. V. Antipov, N. R. Khasanova and S. S. Fedotov, *IUCrJ*, 2015, **2**, 85–94.

6 M. E. A. y de Dompablo, U. Amador and J. M. Tarascon, *J. Power Sources*, 2007, **174**, 1251–1257.